

**International Advanced School on
WIND-EXCITED AND AEROELASTIC VIBRATIONS
OF STRUCTURES**

Genoa, Italy, June 12-16, 2000

BLUFF-BODY AERODYNAMICS

Lecture Notes

by

Guido Buresti

*Department of Aerospace Engineering
University of Pisa, Italy*

1 – GENERAL CHARACTERISTICS OF FLUIDS AND OF THEIR MOTION

Classical fluid dynamics is based on the assumption that the behaviour of fluids may be described by considering them as continuous media, i.e. without taking the motion of their single molecules into account. This implies that when we define the value of a physical quantity (like density, velocity etc.) at a certain point P in space, we are actually referring to the average value of that quantity within a small volume δv , whose center of gravity is P . This volume must be sufficiently small to be considered infinitesimal with respect to the spatial variations of the macroscopic quantities; on the other side, it must be large enough to contain a number of molecules that is sufficiently high to allow the average value of each quantity, calculated considering all the molecules of the volume, to be statistically stationary. In practice, all these conditions are easily verified even with very small dimensions of δv . For instance, in normal temperature and pressure conditions, a volume of air of 10^{-9} mm^3 contains approximately 2.7×10^7 molecules. From the macroscopic point of view, the volume δv may then be considered as infinitesimal, and treated as a material point, which is referred to as a “*fluid particle*”.

The physical properties that characterize fluids (and distinguish them from solids) are the lack of a definite shape and the possibility of finite deformation even under the action of infinitesimal forces, provided the latter are properly applied. More precisely, a fluid may be defined as a substance that deforms continuously under the action of tangential stresses. Conversely, when no motion is present, i.e. in conditions of static equilibrium, a fluid particle is subjected only to normal stresses (which are called *pressure* stresses), and not to tangential stresses (at variance with what may happen for solids).

Fluids comprise both *liquids* and *gases*, but this distinction is much less fundamental from the dynamical point of view. The main difference between them lies in their elasticity, or *compressibility*. Indeed, gases may be compressed much more easily than liquids, so that any motion that implies significant variations in pressure produces much larger variations in density for gases than for liquids. Usually, liquids may be considered with sufficient approximation as incompressible, so that, if ρ is the density, their “*equation of state*” may simply be written as $\rho = \text{constant}$. Conversely, the equation of state of gases is more complex, and links the variation of density to those of the pressure, p , and absolute temperature, T , (considered as thermodynamical state functions). In most cases of practical interest, air may be considered as a “*perfect gas*”, governed by the following well-known equation of state:

$$p = \rho RT \quad (1.1)$$

where R is the characteristic constant of the gas (for dry air $R = 287 \text{ m}^2/(\text{s}^2\text{K})$).

However, it is important to point out that the variations in density of a gas in motion with velocity V become significant only if V is comparable with the “speed of sound”, a , which is the velocity of propagation of small perturbations in the fluid. It may be shown that for a perfect gas the speed of sound is a function of temperature only, through the following relation:

$$a = \sqrt{\gamma RT} \quad (1.2)$$

where γ is the ratio between the specific heats at constant pressure and volume of the gas (for air $\gamma = 1.4$). For air at the pressure of one atmosphere and $T = 15^\circ\text{C}$ (standard conditions), we have $a \approx 340$ m/s.

The parameter characterizing the effects of compressibility is then the Mach number:

$$M = V/a \quad (1.3)$$

It may be shown that the relative variations of density are of the order of $1/2M^2$, so that when M is sufficiently below unity (e.g. $M \approx 0.3$) a gas behaves, with good approximation, as if it were incompressible, and this implies a significant simplification of the equations of motion. Therefore, considering that we are interested here in the evaluation of the aerodynamic loads induced by the wind on civil structures, in the following the fluid will always be assumed to be incompressible.

As already pointed out, a fluid particle in static conditions is subjected only to normal stresses. However, when in motion, a fluid particle is in general also subjected to tangential stresses, which are linked to its tendency to resist deformation, and in particular distortion. This property of the fluid, which is called *viscosity*, is connected to a physical mechanism acting at the molecular level. More precisely, when two adjacent gas particles move with different velocities, the molecules contained in them may migrate from one to the other due to their random thermal motion (which is superposed on their average velocity), thus producing a continuous transport of momentum between the particles.

Due to its motion, the particle is thus subjected to a viscous stress tensor, which acts in addition to the thermodynamic pressure normal stress, and which has both tangential and normal components; the effects of the latter may often be neglected in comparison with those of the pressure stresses. The so-called Newtonian fluids are those for which the viscous stress tensor is assumed to be linearly proportional to the velocity of deformation tensor. In mathematical terms, if τ_{ik} are the components of the stress tensor, and u_i the components of the velocity vector, one has for an incompressible fluid:

$$\tau_{ik} = \mu \left(\frac{\partial u_i}{\partial x_k} + \frac{\partial u_k}{\partial x_i} \right) \quad (1.4)$$

where μ is the *viscosity coefficient*, which is a function of the type of fluid and, in general, of the temperature.

If the fluid may be considered incompressible, i.e. if it is in motion at low Mach numbers, it can be shown that the temperature variations due to the motion are extremely small, so that the viscosity coefficient (which depends approximately on the square root of the absolute temperature) may be considered to be constant. This fact gives rise to a considerable simplification in the equations of motion.

2 – THE EQUATIONS OF FLUID MOTION

The equations of fluid dynamics may be obtained by expressing in mathematical terms the three fundamental balances of the mechanics of continua, viz.

- The conservation of mass (or continuity equation);
- The momentum balance (or fundamental Newton law);
- The balance of energy (or first principle of thermodynamics).

All these balances must obviously be specialized to the particular fluid in exam by appropriate constitutive equations (equations of state, equations for the stress tensor as a function of the velocity components, equations for heat flux as a function of the temperature). Furthermore, they must be referred to a volume of fluid composed always of the same particles (“*material volume*”), which changes position and shape during the motion. However, they may easily be expressed also by considering a fixed control volume.

The equations may be written both in integral form and in differential form. Although for the solution of particular problems the integral form may be more appropriate, the equations of motion are normally used in differential form. The complete set of equations thus obtained is known as *Navier-Stokes equations*, although this term should more precisely refer only to the momentum equations.

As the momentum balance gives rise to a vector equation, a total of five scalar equations may thus be derived. For an incompressible fluid the fundamental unknowns in the equations are the pressure p , the three components of the velocity vector \vec{V} (which in the following will be called u , v , and w , respectively in the x , y and z directions), and the temperature T . However, it is easy to see that if the viscosity coefficient is assumed to be constant (which, as already pointed out, is consistent with the assumption of incompressibility) the temperature is no longer present in the balances of mass and momentum, which then become four equations for the four unknown quantities p , u , v , and w . Once these are obtained for each point in the flow, the components of the stress tensor may be derived from relations (1.4), and the forces acting on any surface (as for instance the surface of a body immersed in the fluid) may be easily obtained by integration of p and τ_{ik} . The equation of energy becomes then an equation for the (slightly variable) temperature field, to be solved after the remaining unknowns are obtained. This is the reason why in the application of the dynamics of incompressible fluids to the derivation of the loads acting on bodies the energy equation is almost never used, and this will also be the case in the following¹.

¹ However, it should be pointed out that the balance of energy cannot be neglected in the study of the large-scale motions of the atmosphere, as well as in all cases in which the presence in the flow domain of significant temperature gradients plays a fundamental role in the production of motion.

Equation of continuity

With the assumption of incompressibility it may be shown that the conservation of mass for a fluid particle is expressed by the following linear differential equation

$$\operatorname{div} \vec{V} = \frac{\partial u}{\partial x} + \frac{\partial v}{\partial y} + \frac{\partial w}{\partial z} = 0 \quad (2.1)$$

The physical meaning of (2.1) becomes clear by recalling that $\operatorname{div} \vec{V}$ corresponds to the relative variation of volume of a fluid particle in unit time.

Momentum balance

The equation for the balance of momentum of an incompressible fluid, in vector notation, is the following:

$$\frac{\partial \vec{V}}{\partial t} + \vec{V} \cdot \nabla \vec{V} = \vec{f} - \frac{1}{\rho} \nabla p + \nu \nabla^2 \vec{V} \quad (2.2)$$

where \vec{f} is the volume force per unit mass acting on the particle, $\nu = \mu/\rho$ is the so-called *kinematic viscosity* of the fluid, and ∇^2 is Laplace's operator.

Equation (2.2) is an expression of Newton's law written in the form $\vec{a} = \vec{F}/m$. Indeed, the two terms in the left-hand side may be shown to express the variation in time of the velocity of a fluid particle, i.e. its acceleration; the first one is the so-called *unsteady term* (which vanishes for steady conditions, in which the various quantities do not depend explicitly on time), while the second is the *convective term*, giving the variation of velocity of a particle due to its transport by the velocity field through a gradient of velocity. In the right-hand side, all terms are forces per unit mass acting on the particle: the first corresponds to volume forces (like gravity), and the remaining ones to the resultant of the surface forces, divided in two terms corresponding one to pressure and the other to the viscous stresses.

For the component of eq. (2.2) in the x_i direction one has:

$$\frac{\partial u_i}{\partial t} + \vec{V} \cdot \nabla u_i = f_i - \frac{1}{\rho} \frac{\partial p}{\partial x_i} + \nu \nabla^2 u_i \quad (2.3)$$

The problem is completed by the initial conditions for unsteady flow and by the boundary conditions. The former prescribe that at the initial time the values of all the unknowns must be given in the whole field. As for the boundary condition on solid walls, the relative velocity between wall and fluid must be zero (no-slip condition); thus the fluid velocity vanishes if the wall is at rest. This condition describes with excellent approximation the behaviour of viscous fluids, and is one of the main mechanisms influencing the pattern of the whole flow field, but is also the source of many of the difficulties in the solution of the Navier-Stokes equations.

Indeed, with the exception of very particular cases, these equations may not be solved in closed form due to their non-linearity, deriving from the convective term.

However, if the bodies immersed in the fluid have certain geometrical characteristics and move (or are immersed in a freestream) with adequate orientations, then it may be possible to devise physical schemes of the problem leading to a simplified mathematical formulation, which still takes the essential physics into account. As will be made clear in the following, this is what happens for the so-called *aerodynamic bodies* (like the wings of an airplane). However, this is normally not the case for most civil structures immersed in the wind, which fall in the category of *bluff bodies*, and for which resort must be made either to experiments or to the numerical solution of the equations of motion. Due to the rapid increase in computer power, the latter is a strongly developing research field; however, for the moment it is not possible to solve the complete set of equations for the flow conditions of most practical applications without using some sort of modelling of the problem; the available codes must thus be used with caution in the design of structures. Consequently, for these cases experiments are still the most important source of information.

3. VORTICITY AND THE SIMPLIFICATION OF THE EQUATIONS OF MOTION

In order to better clarify the importance of the geometrical shape on the possibility of carrying out a theoretical approach, it is appropriate to further analyse some physical and mathematical aspects of the problem. To this end, it is useful to introduce the *vorticity* vector:

$$\vec{\omega} = \text{curl}\vec{V} = \nabla \times \vec{V} \quad (3.1)$$

From the definition, it may be seen that in quite general conditions the velocity field may directly be derived from the knowledge of the vorticity field. It is also easy to show that the value of the vorticity in a point is equal to twice the angular velocity of the fluid particle occupying that point. More importantly, it is not necessary that this quantity be present in the whole field, and its distribution and dynamical behaviour determines the values of the forces acting on bodies immersed in the fluid. Finally, by introducing vorticity, the equations of motion may be given a form that may be very useful to understand the role of the various terms and to devise solution procedures.

Indeed, if V is the modulus of the velocity vector, the following vector relations apply:

$$\vec{V} \cdot \vec{V} = \vec{\omega} \times \vec{V} + (V^2 / 2) \quad (3.2)$$

$$\nabla^2 \vec{V} = -(\text{div}\vec{V}) - \text{curl}\vec{\omega} \quad (3.3)$$

If we now take eq. (2.1) into account, and assume the volume forces to be conservative, i.e. that they may be derived from a potential so that $\vec{f} = -\nabla\phi$, by introducing the above relations into eq. (2.2) we obtain immediately the following fundamental equation:

$$\frac{\partial \vec{V}}{\partial t} + \vec{\omega} \times \vec{V} = - \left(p / \rho + V^2 / 2 + \right) - \nu \text{curl} \vec{\omega} \quad (3.4)$$

This form of the equation of motion is particularly important, because it allows the conditions of validity of widely-used relations to be highlighted.

First of all, it may be seen that if the motion is *irrotational*, i.e. with zero vorticity, or even if $\text{curl} \vec{\omega} = 0$, then the last term in the equation, connected with viscosity, vanishes. It should be pointed out that this does not mean that the viscous stresses are zero, but that their resultant force per unit volume acting on a particle is zero. The consequence is that the equation of the irrotational motion of a viscous incompressible fluid coincides with the equation of motion of an *inviscid* fluid, i.e. a fluid in which the viscous stress tensor is zero and only pressure forces act on the fluid particles.

If the motion, besides being irrotational, is also steady, then the first term in (3.4) also vanishes, and *Bernoulli* equation holds in the field:

$$p / \rho + V^2 / 2 + \quad = \text{constant} \quad (3.5)$$

Furthermore, it follows immediately from definition (3.1) that the condition of irrotationality implies that

$$\vec{V} = \nabla \phi \quad (3.6)$$

where the scalar function ϕ is the *velocity potential*.

By introducing relation (3.6) into the equation of continuity (2.1), one obtains the following linear equation for the velocity potential

$$\nabla^2 \phi = 0 \quad (3.7)$$

Therefore, the problem is now reduced to solving eq. (3.7) for the velocity potential, deriving the velocity field from (3.6), and then obtaining the pressure field from Bernoulli equation (in which the variation of ν may also often be neglected).

This extremely simplified procedure applies, as already pointed out, when the motion is irrotational. However, it is easy to show that the *completely* irrotational flow of a viscous fluid around a solid body is impossible due to the no-slip boundary condition. Indeed, the latter may be satisfied only through a continuous production of vorticity from the solid boundaries.

Conversely, if the fluid is considered to be inviscid, then it may be seen that the resulting equation (obtained by deleting the last term in eq. (2.2)) requires a boundary condition only for one velocity component; the condition at a solid boundary becomes then that the normal velocity component be zero, while a tangential velocity is allowed. Furthermore, it is easy to show that if the initial condition is irrotational (as for a motion starting from rest) then in a non-viscous incompressible fluid there are no physical mechanisms producing vorticity, so that the irrotational motion is the normal rule.

The assumption of non-viscous fluid (or more precisely, of neglecting the last term in eq. (2.2)), has been the basis of much theoretical work in the 19th century, not only because it leads to a simplified mathematical treatment, but also because it has an apparently strongly logical background even from the physical point of view. Indeed, it may be shown that the ratio between the inertia terms in eq. (2.2) (i.e. those appearing in the left-hand side) and the viscous term is of the order of the *Reynolds number*

$$Re = \frac{\rho UL}{\mu} = \frac{UL}{\nu} \quad (3.8)$$

where U and L are, respectively, a characteristic velocity and a characteristic length of the problem.

Now a rapid evaluation shows that most problems of practical interest (and in particular the evaluation of the aerodynamic forces induced on civil structures by the wind) are characterized by Reynolds numbers of the order of 10^6 to 10^8 . Thus the assumption of inviscid fluid seems to be a quite reasonable one. However, if one now follows the above described simplified procedure and solve eq. (3.7) with the condition of tangential velocity at a solid boundary, a solution exists for the velocity field but corresponds to a pressure distribution which, once integrated around the surface of a body immersed in the flow, gives zero resultant force. This is the well-known *d'Alembert's Paradox*, which is in obvious contrast with practical experience, and has been the source of a long-lasting disagreement between applied mathematicians and engineers. Its origin is obviously in the fact that, even for very high Reynolds numbers, a viscous fluid always satisfies the no-slip boundary condition at a solid wall, and, as already pointed out, this is the source of vorticity and of the fundamental differences between the flow of inviscid and viscous fluids.

4. BOUNDARY LAYERS

The above described theoretical impasse was overcome by Prandtl, who introduced in 1904 the concept of a "*boundary layer*", i.e. of a thin region close to the solid surfaces where the effects of viscosity are felt, and the velocity passes from zero at the wall to the value corresponding to irrotational flow (see Fig. 1). From what has already been pointed out regarding the formulation of the equations of motion, the boundary layer corresponds to the region where vorticity is present near the wall. The extent of this region may be shown to be of the order of $Re^{-1/2}$, so that for sufficiently high Reynolds numbers the thickness of the boundary layer remains small, and the equations of motion may be simplified by using order of magnitude considerations. The fundamental result obtained by Prandtl with this procedure is that the variation of pressure *across* the boundary layer is negligible, which means that the pressure acting on a certain point of a solid wall is approximately the same as that present at the upper border of the boundary layer over the same point.

It is then possible to devise an iterative calculation procedure. At the first step the boundary layer is assumed to be of infinitesimal thickness (or, in other terms, to be squeezed

on the surface), so that equation (3.7) is solved with the non-viscous tangential velocity condition at the wall. The resulting pressure distribution is then used as an input to solve the boundary layer equations; this step is not as straightforward as solving the linear Laplace equation, but procedures of different complexity and approximation are available (particularly for the two-dimensional case) and may easily be implemented in relatively-inexpensive numerical codes. Outputs of this step are the tangential stresses acting at the wall and the evolution of the boundary layer thickness over the surface. The former may be integrated to obtain a first evaluation of the friction drag acting on the body, while the latter is used as input for the second potential-flow calculation. In practice, the thickness of the boundary layer is superposed on the original body surface², and equation (3.7) is solved for the flow around the modified body. A second pressure distribution is thus obtained, which may be shown to give rise, when integrated over the body surface, to a non-zero force in the direction of the freestream (drag force), thus overcoming d'Alembert's Paradox. Furthermore, the procedure may then be iterated, and the new pressure distribution used as an input to another boundary layer calculation; the process is ended when two successive results (in terms of the quantity of interest) are sufficiently close.

This procedure may be used in all cases in which the above described physical scheme is valid, i.e. when a thin vorticity-containing boundary layer contours the whole body surface and joins downstream to form a thin wake. This comprises, for instance, most configurations of interest for aeronautical engineering. However, it is unfortunately not the general case, and when the body shape is such that the perturbation it produces on the flow gives rise to accelerations followed by sufficiently strong decelerations, a phenomenon known as “*boundary layer separation*” occurs (Figs. 2 and 3). Indeed, when the velocity outside the boundary layer decreases, the pressure consequently increases, as follows from Bernoulli equation. As the pressure is constant across the boundary layer thickness, all particles within it are subjected to the same pressure gradient force. Consequently, the lower-momentum particles near the solid surface undergo a relatively larger deceleration, the boundary layer velocity profile changes its shape with the appearance in it of an inflexion point, and, finally, a limit condition is reached beyond which the flow changes direction near the wall, moving upstream. This is the separation point, characterized in two-dimensional conditions by the vanishing of the derivative of the tangential velocity component in the direction normal to the surface. Beyond this point, the irrotational flow moves far away from the wall, and the region where vorticity is present is no longer thin and close to the body surface. Conversely, vorticity fills up all the downstream separated region, forming a wake characterized, in general, by significant velocity fluctuations, i.e. by unsteady flow conditions. It is obvious that the boundary layer approximations and results cannot be applied beyond separation (and actually even slightly before it), and the whole physical scheme leading to the previously-described simplified solution procedure for the equations of motion is no longer valid.

It must be recalled at this point that boundary layers may also undergo another fundamental phenomenon, viz. transition to the *turbulent* state. Indeed, when the Reynolds

² Actually, the so-called *displacement thickness* is used, which corresponds to the distance through which the outer irrotational flow is displaced by the retardation of fluid inside the boundary layer.

number based on the distance from the front stagnation point on a body (which may be considered as the starting point for the boundary layer development) is sufficiently low, then the flow is in the *laminar* condition, in which the fluid particles move one over the other in steady layers. However, when the Reynolds number exceeds a certain critical value, then the laminar flow becomes unstable to perturbations, and, after a transition region, a new condition is developed in which the fluid particles have random fluctuations superimposed on their mean velocity. A visualization of a turbulent boundary layer is shown in Fig. 4. The critical Reynolds number value may be of the order of 10^5 , but this value strongly depends on various parameters, like the wall surface roughness, the presence of fluctuations or turbulence in the incoming stream, the value and sign of the pressure gradient along the surface.

As a result of the larger mixing between the various layers of fluid that is produced by the macroscopic migration of fluid particles (at variance with what happens for the viscous momentum transport, which occurs at the microscopic level), turbulent boundary layers are thicker than the laminar ones, and are characterized by an increased value of the tangential stresses at the surface; therefore, turbulent boundary layers give rise to higher friction forces on the bodies. However, the larger energy content inside turbulent boundary layers has also the consequence that they are much more resistant to separation than laminar boundary layers, i.e. they are capable of remaining attached to the surface for larger adverse pressure gradients or for a greater surface extension for the same value of the pressure gradient (see Fig. 5). Nevertheless, it must be pointed out that all types of boundary layers, laminar or turbulent, separate at sharp edges, so that the difference in behaviour with respect to separation between the laminar and the turbulent conditions may be observed only for bodies with curved surfaces, i.e. without sharp corners. Finally, it must be noted that the basic boundary layer assumptions and results (and in particular the constancy of pressure across the thickness) still apply also for turbulent boundary layers.

We may now proceed to a classification of bodies with respect to the features of the flow field they produce when they are immersed in a cross-stream (or are moving through still fluid). We will call "*aerodynamic bodies*" those characterized by thin boundary layers completely attached over their whole surface, which leave behind them thin and generally steady wakes containing vorticity. The aerodynamic forces acting on these bodies may be evaluated through the previously described simplified potential flow - boundary layer procedure. Conversely, "*bluff bodies*" are characterized by a more or less precocious separation of the boundary layer from their surface, and by wakes having significant lateral dimensions and normally unsteady velocity fields. As already pointed out, for these bodies no simplified mathematical treatment is usually possible, and the forces acting on them may be evaluated either from the solution of the complete Navier-Stokes equations or from the results of ad hoc experiments.

As is apparent from Fig. 6, the type of flow occurring is defined not only by the shape of the body but also by its orientation to the flow, and any aerodynamic body may become a bluff body for certain free-stream directions.

Obviously the above classification is a crude one, particularly as regards bluff bodies. Actually, one might further distinguish between bodies having different "degrees of

bluffness”, for instance by referring to the ratio between the cross-flow dimensions of the separated wake and of the body, or to the extent of the body surface immersed in the separated wake. Indeed, these distinctions may have sense, particularly as regards their bearing on the consequent forces acting on the body. Nevertheless, as will be explained in the following, it is again the *type* of flow the bodies produce in their wakes, particularly as regards the amount and level of organization of the vorticity field, that has the greatest importance both from the aerodynamical and from the design points of view.

5. AERODYNAMIC LOADS ON BODIES

5.1. General considerations

The loads acting on a body immersed in a flowstream are produced by the normal and tangential stresses over its surface. When integrated, these stresses give rise to the resultant load components, which are usually expressed in non-dimensional form by means of *force and moment coefficients*, defined as follows:

$$C_{F_i} = \frac{F_i}{\rho U^2 S} ; \quad C_{M_i} = \frac{M_i}{\rho U^2 S l} \quad (5.1)$$

where F_i and M_i are the components in the x_i direction of the resultant force and moment acting on the body, U is the undisturbed upstream flow velocity, S is a reference surface and l a reference length. In the case of two-dimensional bodies (which approximately represent sufficiently long structural elements), the load coefficients are defined by using the load per unit distance along the span of the body in the numerator, and a reference length in the denominator (which is normally either the cross-flow or the along-flow dimension of the body cross-shape).

It is often useful to refer also to the pressure p acting at a certain point of the body surface, by using a *pressure coefficient* defined as

$$C_p = \frac{p - p_\infty}{\rho U^2} \quad (5.2)$$

where p_∞ is the pressure in the undisturbed upstream flow.

The above mentioned loads have, in general, mean and time-varying components (which may be characterized, e.g., by their r.m.s. values and by their frequency spectra). The fluctuating loads may be significant not only when the upstream flow is time-dependent (for instance due to the presence of turbulence), but also when the wake produced by the body itself has more or less regular fluctuations. In general one may say that, for steady upstream flow, aerodynamic bodies are characterized by steady wakes and loads, whereas for bluff bodies the opposite is true.

5.2 Two-dimensional bodies

One of the most important force components is the drag, i.e. the component of the aerodynamic force in the upstream flow direction (or in the direction of motion of the body if this is moving in still fluid). One striking difference between aerodynamic and bluff bodies is that the former have drag coefficients that are at least one order of magnitude smaller than the latter. This is due to the remarkable increase in pressure drag deriving from the boundary layer separation.

Indeed, the flow field around aerodynamic bodies is not very different from that corresponding to non-viscous potential flow, apart from the displacement effect of the boundary layer. Therefore, the pressure distribution is also only slightly different from the ideal one which, as already pointed out, integrates to a zero value (d'Alembert's paradox); consequently, the pressure in the aft part of the body returns to values not very far from those acting on the front part, and the resulting pressure drag is thus rather small. Apart from particular cases, the main contribution to the drag of an aerodynamic body derives then from the integration of the tangential viscous stresses (*friction drag*).

The situation is completely different for a bluff body, because separation prevents the occurring of the recompression in the rear part of the body, so that the values of the pressures in this region are considerably smaller than those acting in the front part (and correspond normally to negative pressure coefficients). This gives rise to a significant value of the *pressure drag*, which is normally much higher than the friction drag, such that the latter (which remains of the same order as that of an aerodynamic body) may often be neglected.

More in detail, the pressure drag may be divided in two contributions, respectively given by the *forebody*, i.e. the front part of the body with attached boundary layer, and by the so called *afterbody* or *base* region, i.e. the portion of the body surface lying inside the separated wake. Depending on the shape of the forebody, the first contribution may be large or small, as can be seen by comparing the qualitative pressure distributions around a flat plate and a circular cylinder (see Fig. 7). The second contribution, on the other hand, is determined by the value of the suction³ acting on the base, which are primarily connected with the velocity outside the boundary layer at the separation point, V_s . Indeed, particularly in the case of afterbodies with limited longitudinal extent, the pressures on the base are almost constant, and equal to the pressure in the outer flow at the separation point. In terms of pressure coefficient, by using Bernoulli's equation one has

$$C_{ps} = 1 - V_s^2 / U^2 \quad (5.3)$$

Therefore, the higher is the velocity outside the boundary layer at the separation points, the lower is the base pressure, and the higher the base drag.

Particularly important is the dependence of the drag coefficient of a bluff body on the Reynolds number. As can be seen from Fig. 8, while for bodies with sharp corners this dependence is negligible, it becomes more and more significant with the rounding of the

³ Obviously, pressures act always towards the body surface, but the term *suction* is often used when the difference ($p-p_\infty$) is negative.

body, with the appearance of a sudden decrease of the drag coefficient. This behaviour is connected with the phenomenon of transition of the boundary layer to the turbulent state, which, as already pointed out, is more resistant to separation than the laminar one. Therefore, for bluff bodies without sharp corners, a critical value of the Reynolds number exists which corresponds to transition taking place before the laminar separation, so that the separation points move downstream, a narrower wake forms, a higher pressure recompression before separation takes place, and a consequent significant decrease of the drag coefficient is observed. Obviously, all parameters that may influence the boundary layer transition (as the incoming turbulence level and the surface roughness of the body) have a significant influence on the C_D-Re curve, and produce a variation of the critical Reynolds number. This implies, for instance, that for motions in certain ranges of Reynolds numbers, a rough surface may be advantageous to reduce the drag of the body.

The drag force acting on a body may also be given an interpretation in energetic terms. Indeed, the work done in a certain time interval by the drag force is equivalent to the variation in the total energy (i.e. the sum of the internal and kinetic energies) of the whole fluid field in the same time interval. This variation may be seen to be strictly connected with the amount of perturbation energy present in a section of the wake downstream of the body. Thus the different values in drag of different bodies may be related to differences in the energy content in their wakes. This type of reasoning, although obvious to a certain extent, is actually extremely fruitful not only to justify different values of drag, but also to give a rationale for any design action aimed at obtaining a drag reduction of a body.

Figure 9 shows the different dimensions of an airfoil (an aerodynamic body) and of a circular cylinder (a bluff body) which experience the same drag force when immersed in a freestream at the same velocity. The striking difference in size between the two bodies is due to the fact that value of the drag coefficient of the first one is 15 to 20 times smaller than that of the second. The reason for this is immediately clear when one compares the different flow fields connected with the two bodies (Fig. 10). Indeed, the airfoil leaves behind it an extremely thin wake deriving from the joining of the upper and lower boundary layers over its surface (and comprising the momentum defect due to the flow retardation caused by the viscous no-slip boundary condition). Consequently, this flow configuration gives rise to a very small perturbation energy. The opposite is true for the circular cylinder, which shows a highly-energetic wake, characterized by the presence of a double row of alternate concentrated vortices (known as *Karman vortex street*). This vortex shedding phenomenon is typical of all two-dimensional bluff bodies, and has a great practical importance. Indeed, it is the source of oscillating cross-flow forces that may induce significant oscillations of a structure if their frequency coincides with one of the natural frequencies of the structure. A detailed review on the phenomenon of vortex shedding, on the consequent induced forces, and on the effects of the variation of geometry and of various fluid dynamical parameters may be found in Buresti (1998).

The main point that will be made here is that a strict connection exists between the amount of perturbation energy and the organization of the vorticity present in the wake. Indeed, the drag of a bluff body is an increasing function of the degree of concentration in space of the

vorticity shed in its wake, and of the distance between the regions where the positive and negative vorticities are contained. The reason for this fact may be understood from Fig. 11, in which the velocity fields corresponding to two rigidly-rotating vorticity cores, having the same global value of vorticity but different radius, are compared. By recalling that the vorticity in each point of the core is equal to twice its angular velocity of rotation, it can be derived that the maximum velocity induced by this ideal type of vortex is inversely proportional to the radius of its core. The fact that actually vorticity is not exactly constant inside a real vortex core does not change the qualitative conclusion drawn from this example. It is also easy to see that, if one considers two vortices of different sign, the global kinetic energy connected with the associated velocity field increases with the distance between the two vortices.

The same results are obtained also by considering the general theory of Wu (1981), which connects the aerodynamic drag experienced by a body with the variation of the axial moment of vorticity that it produces. Incidentally, a further important result of this theory is that, if a body moves in steady rectilinear motion in an incompressible viscous fluid, the total amount of vorticity present around the body surface and within the fluid is always constant, i.e. it is zero if the motion started from rest. This implies that the instantaneous total amounts of positive and negative vorticity are equal.

By applying the above considerations to two-dimensional bluff-bodies, one understands why their drag increases with the width of their wakes (due to the larger distance between oppositely-signed vorticity) and is connected with the presence of regularly-shed concentrated vortices. However, a further consequence is that one may reduce the perturbation energy (and thus the drag) of a bluff body (without significantly changing the width of its wake) by preventing the vorticity from concentrating in restricted cores. This may be obtained by interfering with the vortex-shedding process, for instance by avoiding the occurrence of the separation of the boundary layer along a straight line (which may be seen to be a necessary condition for regular vortex shedding to take place). To this end, various types of protuberances may be positioned along the span of the body (Fig. 12), or, if possible, more drastic variations of the body contour may be used (Fig. 13). By these means drag reductions as high as 50% may be obtained. Obviously, the inhibition of vortex shedding has also the positive effect of avoiding the consequent fluctuating cross-flow forces and the related oscillatory phenomena. Further details on drag reduction may be found in Buresti (1998).

Bluff bodies are obviously also subjected to forces in the across-wind direction and to moments around the various axes due to non-symmetries of the pressure distribution on their surface. Therefore, these loads depend fundamentally both of the body shape and on the orientation of the incoming freestream. Particularly in the two-dimensional case, the force component in the across-wind direction is often called lift force, in analogy to the corresponding force acting on an aeronautical wing section (airfoil). It is interesting to recall briefly the physical origin of lift on a wing, which is due to the downward deflection that the airfoil induces on the flow when moving at relatively small values of the angle of attack (the angle between the freestream direction and the direction of symmetrical flow). This effect is strictly connected with the shape of the airfoil (which, as already seen, in our definition is an

aerodynamic body), and in particular with the fact that it is characterized by a sharp trailing edge. If we imagine starting the airfoil impulsively from rest, it can be seen that, due to the nonsymmetrical flow configuration of the potential flow field that is initially induced by the motion, streamlines tend to round the trailing edge. However, due to the presence of the sharp corner, the boundary layer separates there, and a starting vortex, containing vorticity of only one sign, is left in the flow. During the initial stages of motion the starting vortex is rapidly carried away from the airfoil, so that its effects are no longer felt, and the flow around the airfoil becomes the already described one, typical of an aerodynamic body, with attached boundary layers all over its surface. However, a surplus of vorticity of sign opposite to that of the starting vortex, but having the same absolute value, remains around the airfoil, and causes the flow passing over its upper surface to accelerate and the flow passing over its lower surface to decelerate. This velocity difference produces a pressure difference (with lower relative pressures on the upper side and higher relative pressures on the lower side), and a resultant upward force. Thus the mechanism producing lift is seen to depend in an essential manner on viscosity, and on the separation of the boundary layer at the sharp trailing edge during the initial stages of the motion.

Coming back to bluff bodies, the above described mechanism does not apply in all its details, particularly because the boundary layer cannot remain attached to their surface even after the end of the initial transient. However, if the body is sufficiently elongated (like an ellipse), a starting vortex is shed anyway (even if not as strong as that of an airfoil), and the asymmetry of the final flow configuration for non-symmetrical wind orientations may be sufficient for producing significant lateral forces. On the other hand, bodies with an upstream flat face normal to the wind direction and bounded by sharp corners (like those having square or non-elongated rectangular cross-sections) are characterized by complex asymmetrical flows, and for certain wind orientations they may be subjected to mean cross-flow forces which are in the opposite direction than those acting on elongated bodies. This may produce the oscillatory phenomenon of *galloping*, which may also interfere in a complex way with the oscillations induced by the shedding of vortices. Incidentally, the cross-flow fluctuating forces induced by vortex shedding may be seen as the result of the continuous production of asymmetrical flow around the body during the shedding of each vortex.

5.2. Three-dimensional bodies

In the design of structures immersed in the wind, three-dimensional conditions are most usual, due to the shape of the considered bodies, to the possible non-uniformity of the incoming freestream, or to the occurrence of both these conditions.

The complexity of the flow around a body that might schematically represent a building is shown in Fig. 14. As can be seen, due to the incoming wind boundary layer, in this case flow separations are in general present even upstream of the body, with the consequent formation of “*horseshoe vortices*”, which strongly interact with the lower part of the body. Similarly to what happens in the two-dimensional case, the mean and time-varying forces are fundamentally dependent on the behaviour of the vorticity introduced in the wake.

Due to the complexity and great variety of the possible flow configurations, and the high number of influencing parameters, the present level of knowledge does not allow reliable load predictions to be made for generic cases. Therefore, it is necessary to rely upon experimental data bases relating to common shapes, which permit to cope with various interesting design conditions, but which refer mostly to the mean forces (and often only to drag coefficients).

The first general point that must be made is that, in general, an isolated, low-aspect-ratio three-dimensional body is characterized by lower aerodynamic loads than those acting on a two-dimensional body of analogous cross-shape (Fig. 15). This is, in a sense, reasonable, since the disturbance caused by a three-dimensional body is lower due to the possibility of flow in an additional direction; however, actually the behaviour of the forces is mainly linked to the modifications of the flow structures and of the vorticity field in the separated wake.

For instance, if we consider a finite-length cylinder as in Fig. 16, it is apparent that the low pressure existing in the wake region causes a flow around the free-ends of the body, which penetrates inside the wake, widens it, and moves downstream the rolling up of the vortices detaching from the lateral sides. As a consequence, at variance with what happens in the two-dimensional case, the widening of the wake and the consequent reduction of the vortex shedding frequency occur in this case with a reduction of drag, caused by the increase of the base pressure due to the flow entering the wake, and by the lower value of the perturbation energy induced by the lower-intensity shed vortices.

Figure 16 also shows the appearance of another fundamental structure typical of many finite-length bodies, viz. the two intense longitudinal vortices produced by the confluence of the lateral flow with the flow passing over the free-end. These vortices may produce high local suction on the structure, so that the local drag may be high at the free-end even if the global one may be much lower, with obvious consequences on the position of the resultant and on the overturning moment of a structure resting vertically on a plane. Further information on the effects of the finite-length of a body, or of the variation of the cross-shape and of the incoming flow, may be found in Buresti (1998), with particular reference to the modifications induced on the vortex shedding mechanism.

To have a further example of the possible complexity of three-dimensional flows, it may be interesting to describe the case shown in Fig. 17, even if probably not of paramount importance as regards civil structures placed in the wind. As can be seen, an axisymmetrical body having an inclined base and placed in a freestream along its axis, shows an unexpected trend of the drag as a function of the angle ϕ between the base and the wind. Indeed, by increasing ϕ the drag coefficient first increases almost linearly, and then shows a sudden decrease, after which it remain almost constant up to $\phi = 90^\circ$. The critical value of ϕ is also seen to be difficult to predict, and sensitive to small variations in flow conditions, as apparent from the two different curves shown in Fig. 17, which were obtained in two different wind tunnels (Bearman, 1980).

The same figure schematically shows that this behaviour derives from the existence of two completely different flow regimes. For values of ϕ below the critical one, the vorticity introduced in the wake concentrates in two narrow cores, whose intensity increases with increasing ϕ . However, when the inclination of the base becomes excessive, this configuration

can no longer exist, the vorticity introduced in the wake does not show any organization, and, conversely, is completely and irregularly diffused in the wake. From what has already been repeatedly pointed out, the latter flow configuration corresponds to a much lower perturbation energy than the former, and the drag shows a consequent drastic decrease. This is clear also from Fig. 18 a), in which the high and localized suction induced on the base by the vortices is apparent, as well as the lower and almost uniform suction typical of the diffused-wake configuration.

The interest of this example is first of all in the recognition that bluff-body flows may be characterized by sudden discontinuities when one parameter controlling the configuration is varied, and this makes the extrapolation of experimental data extremely dangerous. But, even more importantly, the understanding of the physical mechanisms causing a certain behaviour of the forces gives the possibility of devising means for the modification, in a favourable way, of the flow configuration. Indeed, the limited stability of the above-described longitudinal vortical structures suggests that, by interfering with their production, it is possible to force the establishment of the diffused-vorticity configuration. As can be seen in Fig. 18 b), this is indeed what may be obtained by introducing in the base region small lateral or transversal plates.

Conical vortical structures similar to those now described are typical of delta wings of supersonic airplanes in low-velocity flight, but also of the upper surface of buildings immersed in a wind having certain orientations (Fig. 19). It is then obvious that also in this case small modifications of the contour of the upper end of the building might avoid their appearance, and the consequent (and potentially dangerous) high local suction.

6. INTERFERENCE EFFECTS

The complexity of the possible flow configurations that may characterize isolated bluff bodies immediately suggests that even more complicated conditions may be found when several bodies are placed close enough for interference effects to become significant.

Considering its relevance to design, the first important point to make is that in many of these situations the asymmetries that may originate in the flow due to interference may produce mean cross-wind forces and different moments of considerable magnitude, even for bodies that do not experience these types of load when isolated, due to their symmetrical geometries. Also the fluctuating forces may be considerably altered by interference, and new coupled instabilities may derive from proximity effects.

Obviously, the opposite may also be true, i.e. certain flow configurations leading to fluctuating loads and high drag, like vortex shedding, may be changed and even suppressed by interference effects. Examples of this are the works of Igarashi (1997) and Prasad & Williamson (1997), who respectively used a small rod placed in front of a square cylinder and a small flat plate placed in front of a circular cylinder to modify the flow field of the downstream body (Figs. 20 and 21). Their results show that the drag of the system of two bodies may be much lower than the drag experienced by the single downstream body when

isolated, and optimal geometrical configurations (in terms of relative distance and ratio between the sizes of the two bodies) may be found producing drag reductions as high as 60%.

Further information on interference effects, particularly as regards two-dimensional bluff bodies, may be found in Buresti (1998). One of the main points arising from the available literature data is that, once again, sudden complete changes in the flow may occur even for small variations of the governing geometrical parameters. Furthermore, bistable flow patterns may exist, i.e. conditions having two possible equilibrium states with different flow configurations (and consequently different aerodynamic loads); the occurrence of any of the two patterns may be triggered by external perturbations, which may then lead to dangerous self-excited oscillations of a flexible body.

Therefore, for bluff bodies in possible interference, the extrapolation of available data is even more dangerous than for isolated bodies; care must then be taken when applying experimental information to cases even slightly different from the tested ones. Nevertheless, it is clear that previous experience and fluid dynamic knowledge may be used to guess the possible influence of the variation of certain parameters (like Reynolds number, freestream turbulence or surface roughness), according to geometry and flow conditions. To this end, it would be essential that experimental campaigns be carried out not only to obtain the loads acting on particular complex geometrical configurations, but also to gather a sufficient data base regarding the interference between commonly-used types of bodies. On this respect, the present situation is not yet satisfactory, and this may also be due to the high number of tests that should be carried out, and to the consequent high cost of such systematic analyses.

The predictive potential given by the availability of good experimental data and by a sufficient competence on the physical mechanisms playing a role in bluff-body aerodynamics may be appreciated from the following example, which will conclude the present notes.

An experimental campaign (Buresti et al. 1986) was carried out to determine the wind-induced loads on a tension leg oil platform, whose upper part is schematically shown in Fig. 22. A 1:250 model of the structure was tested in an aeronautical wind tunnel in which the variable incoming wind profile had been reproduced. The model could be rotated around the vertical axis and the six components of load were measured for wind directions θ from 0° to 360° . The complex trends of the force and moment coefficients obtained as a function of θ are shown in Fig. 23. A detailed analysis shows that several components, and in particular the vertical and lateral forces and the moment around the vertical axis, are significantly higher than could have been predicted without taking interference effects into account.

Particularly important from the design point of view is the variation of the vertical moment M_z as a function of the wind direction, because a tension leg platform is moored to the seabed by a system of pre-tensioned tethers, which gives it a reduced torsional stiffness around the vertical axis. Considering the reference system of Fig. 22, great importance has the derivative of the coefficient C_{M_z} with respect to the wind orientation, because in the ranges of θ characterized by a negative value of this derivative the platform tends to be unstable to rotations around the vertical axis. Therefore, an attempt was made to analyse the possibility of predicting the experimentally-found trend of the vertical moment by adding the four contributions that seemed to be predominating, and in particular:

- a) the moment acting on the main deck considered as a low-rise square prismatic body;
- b) the moment due to the particular shape of two sides of the same main deck, in which a sharp-edge indentation is present;
- c) the moment produced by the lateral forces (due to interference effects) acting on the cylindrical columns supporting the main deck;
- d) the moment due to the drag forces acting on the various bodies placed non-symmetrically above the deck.

The first contribution was estimated by extrapolating the data of E.S.D.U. 1971, for the lateral forces on square-section blocks, and assuming an application point for these forces at 1/3 of the longitudinal dimension. Fig. 24 shows the variation with wind orientation of the resulting contribution to C_{Mz} .

The second contribution was assessed by assuming plausible values for the pressure coefficients acting on the lateral sides of the deck indentations, and is given in Fig. 25.

To evaluate the interference effects between the supporting columns, the two-dimensional data given in E.S.D.U. 1984 and Price & Paidoussis 1984 were used, and the variation of the flow velocity due to the incoming wind profile was taken into account. Figure 26 shows the result of this assessment.

Finally, for the last contribution, the drag of the non-symmetrically placed bodies on the deck was evaluated from the same previous experimental results, as difference between the drag force measured on the complete model and that obtained when each of these bodies was removed. Figure 27 shows the obtained behaviour of this component, which, incidentally, would represent the whole predicted contribution to the vertical moment if only the drag forces had been taken into account (as is sometimes done in certain inadvisable design procedures).

The comparison between the experimental trend of the vertical moment coefficient and the one obtained by adding up the four above described contributions is shown in Fig. 28. As can be appreciated, the agreement is quite good from a qualitative and even from a quantitative point of view. The latter result may be somewhat surprising, considering all the approximation made in the evaluation procedure, and may even be the consequence of compensation effects between opposite inaccuracies. Nevertheless, the fact that the extremely complex trend of the variation of the vertical moment with wind orientation has been closely reproduced, at least as regards the signs of the derivative of the coefficient, suggests that the main contributions to this load component have been taken into account, and that their dependence on θ has been correctly predicted.

The main indication deriving from this example is that, if even approximate data on the forces acting on single bodies of typical shape and on the interference effects between them are available, then satisfactory qualitative and even quantitative predictions of the aerodynamic loads acting on complex structures may be obtained. Unfortunately, as already pointed out, the present information on interference effects, particularly for three-dimensional bodies, is still far from satisfactory, so that, in general, one cannot avoid the recourse to dedicated experimental investigations.

References

- Batchelor G. K., 1967. *An Introduction to Fluid Dynamics*. Cambridge University Press, Cambridge, U.K.
- Bearman P.W., 1980. Bluff body flows applicable to vehicle aerodynamics. *ASME J. Fluids Engineering*, Vol. 102, pp. 265-274.
- Buresti G., 1998. Vortex shedding from bluff bodies. In “*Wind Effects on Buildings and Structures*” (Riera J.D., Davenport A.G., Eds.), Balkema, Rotterdam, pp. 61-95.
- Buresti G., Lombardi G., Montobbio L., Piva R., 1986. Wind tunnel tests on a tension leg platform model. *Proc. 1st ASME-OMAE Specialty Symposium*, pp.485-492.
- E.S.D.U., 1971,. Fluid forces, pressures and moments on rectangular blocks. Engineering Science Data Unit Item N. 71016, (amended 1978).
- E.S.D.U., 1984,. Cylinder groups: mean forces on pairs of long circular cylinders. Engineering Science Data Unit Item N. 84015.
- Igarashi T., 1997. Drag reduction of a square prism by flow control using a small rod. *J. Wind Eng. Ind. Aerodyn.*, Vol. 69-71, pp. 141-153.
- Prasad A. & Williamson C.H.K., 1997. A method for the reduction of bluff body drag. *J. Wind Eng. Ind. Aerodyn.*, Vol. 69-71, pp.155-167.
- Price S.J. & Paidoussis M.P., 1984. The aerodynamic forces acting on groups of two and three circular cylinders when subject to a cross-flow. *J. Wind Eng. Ind. Aerodyn.* Vol. 17, pp. 329-347.
- Simiu E. & Scanlan R.H., 1986. *Wind Effects on Structures*. John Wiley & Sons.
- Van Dyke M., 1982. *An Album of Fluid Motion*. The Parabolic Press, Stanford, California.
- Wu J.C., 1981. Theory for aerodynamic force and moment in viscous flows. *AIAA Journal*, Vol. 19, pp. 432-441.

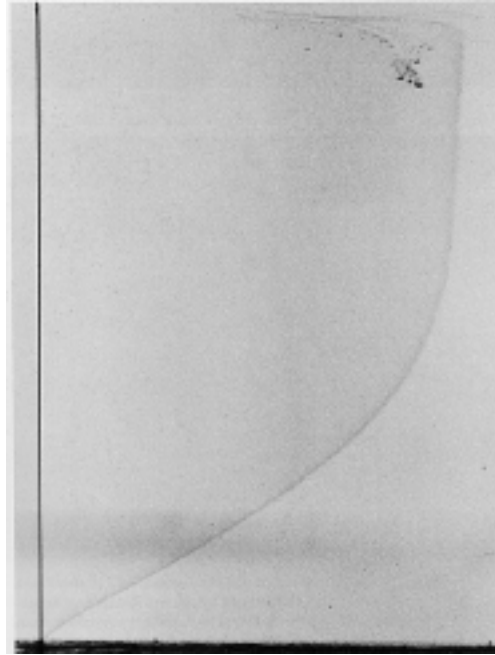


Fig. 1 – Boundary layer profile over a flat plate (from Van Dyke 1982).

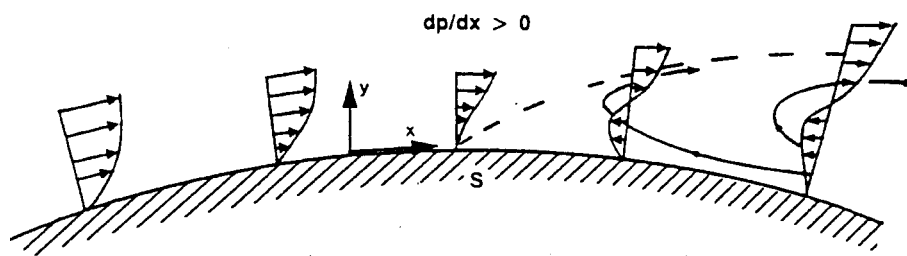


Fig. 2 – Boundary layer separation



Fig. 3 – Example of flow separation from a curved wall (from Van Dyke 1982).

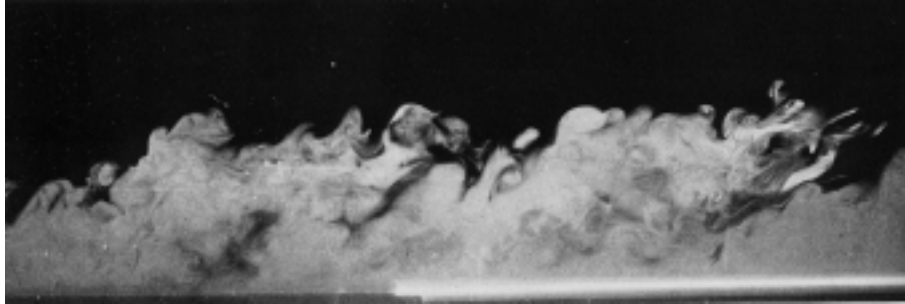


Fig. 4 – Example of turbulent boundary layer visualization (from Van Dyke 1982).

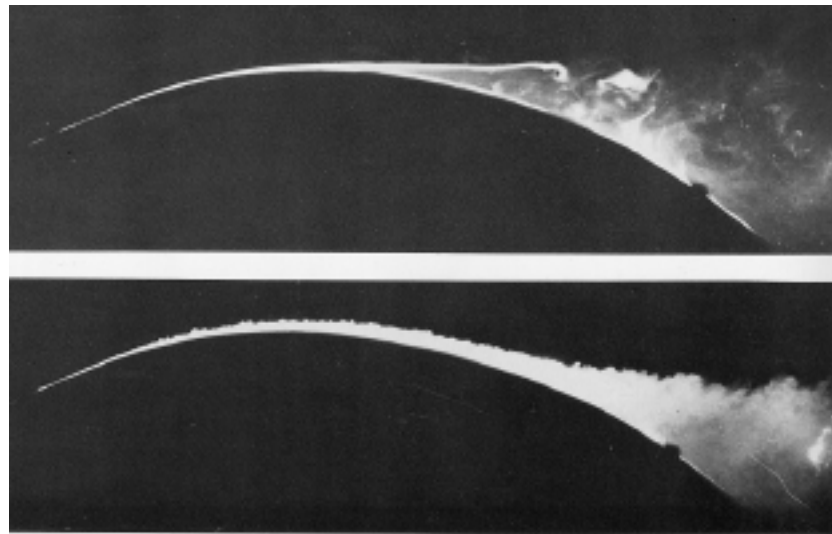


Fig. 5 – Example of laminar (upper photo) and turbulent (lower photo) separation over a curved surface (from Van Dyke 1982).

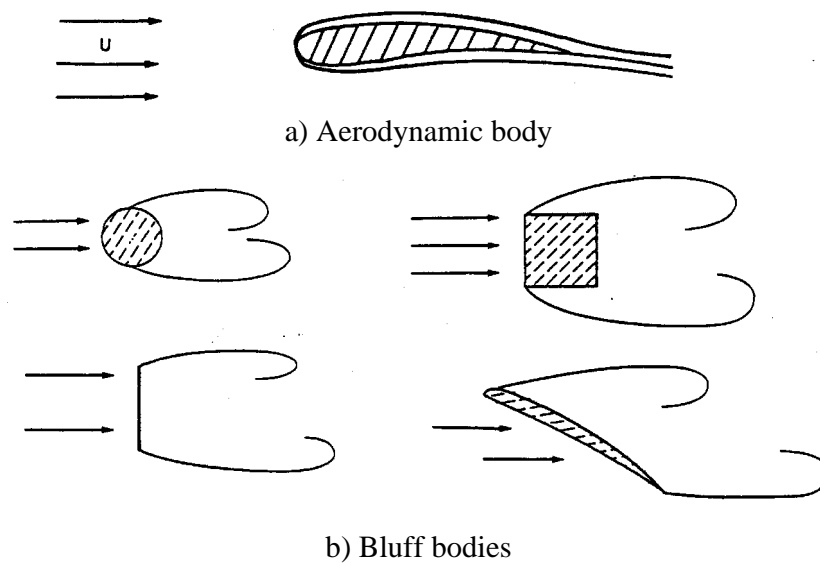


Fig. 6 – Examples of aerodynamic and bluff bodies

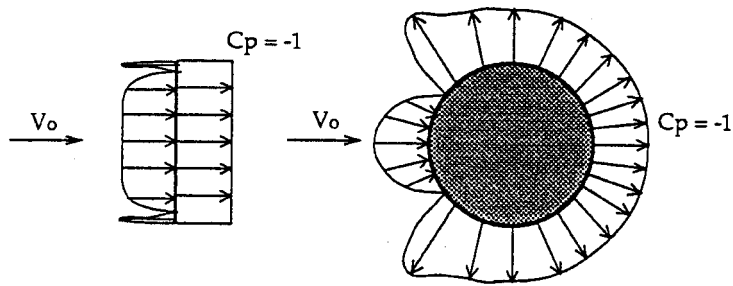


Fig. 7 – Comparison between the pressure distributions of a flat plate ($C_D = 2$) and of a circular cylinder for $Re < 10^5$ ($C_D = 1.2$)

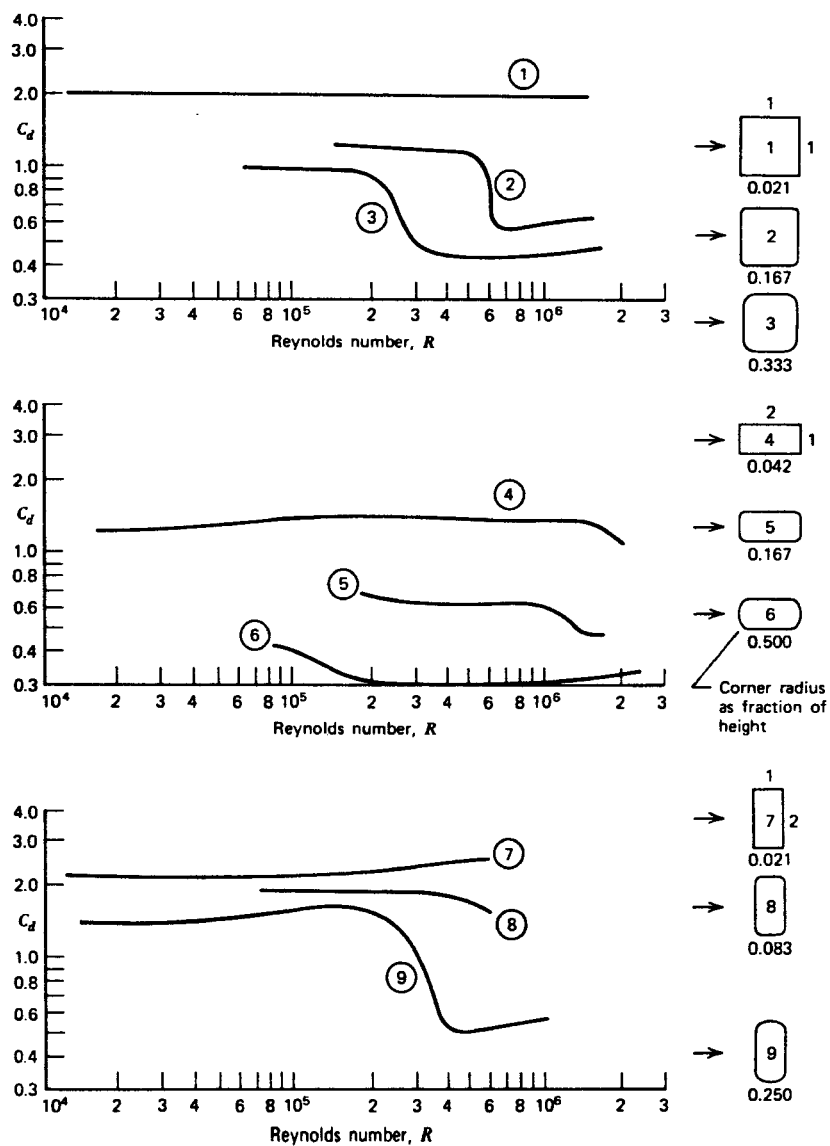


Fig. 8 – Drag coefficients of various cylindrical shapes as a function of Re .

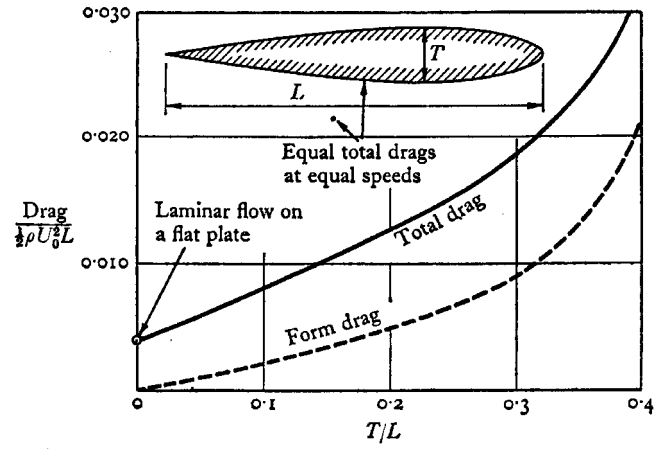
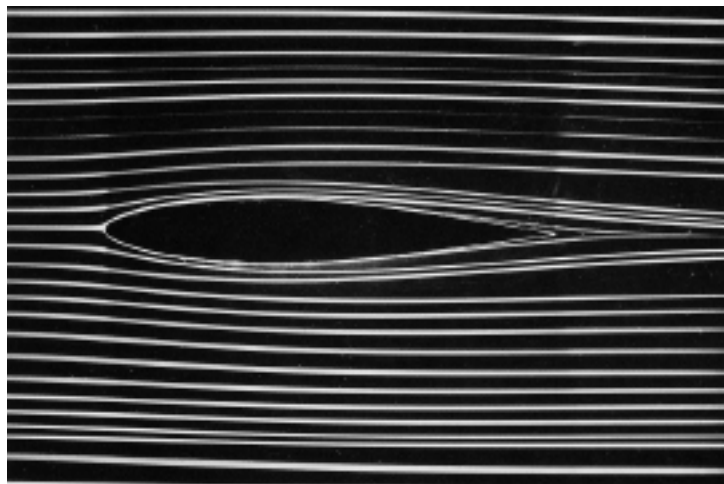
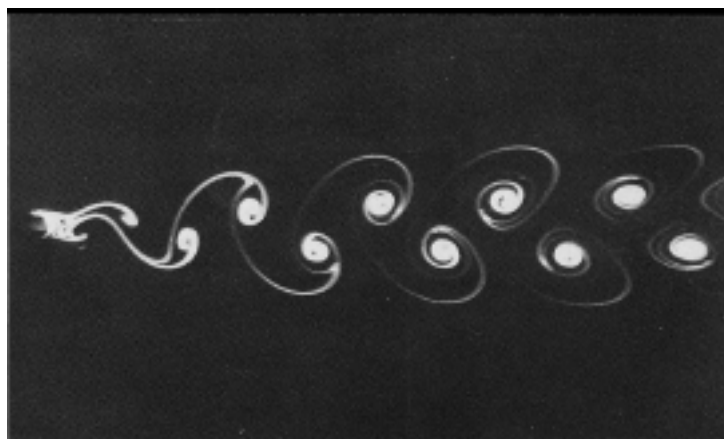


Fig. 9 – Comparison between an airfoil and a circular cylinder having the same total drag (from Batchelor 1967).



a)



b)

Fig 10 – Flow fields around an airfoil and a circular cylinder (from Van Dyke 1982).

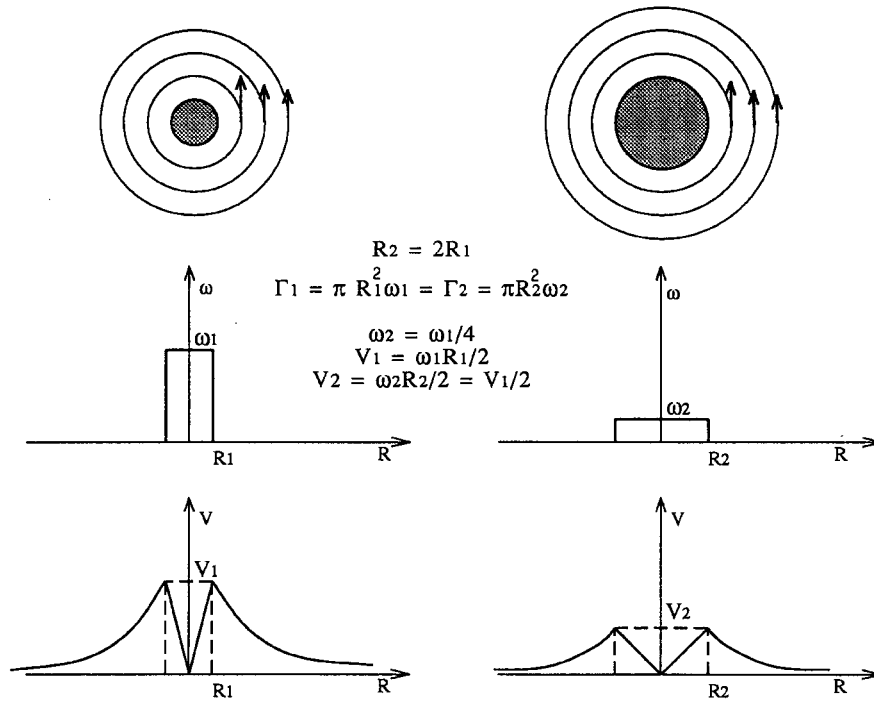
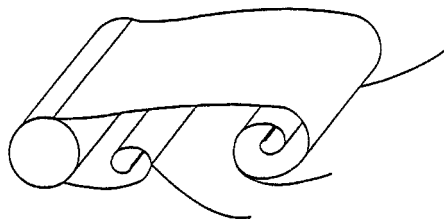
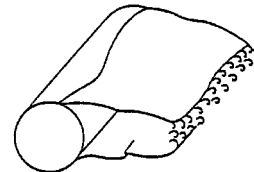


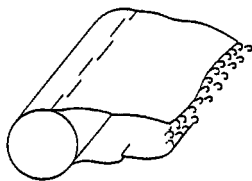
Fig. 11 – Velocity and vorticity fields of two ideal vortices having the same global vorticity but different radius.



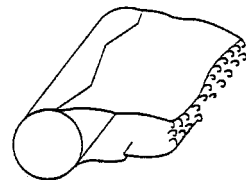
(a) linear separation parallel to cylinder axis



(b) inhomogeneous separation



(c) broken separation wires



(d) corrugated separation wire

Fig. 12 – Influence of separation line on wake structure for a circular cylinder

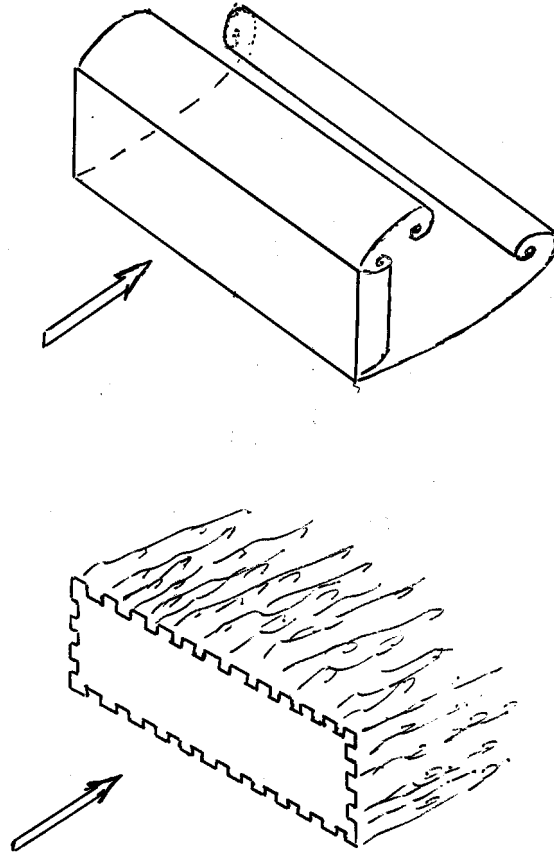


Fig. 13 – Modification of wake structure by serrated contour.

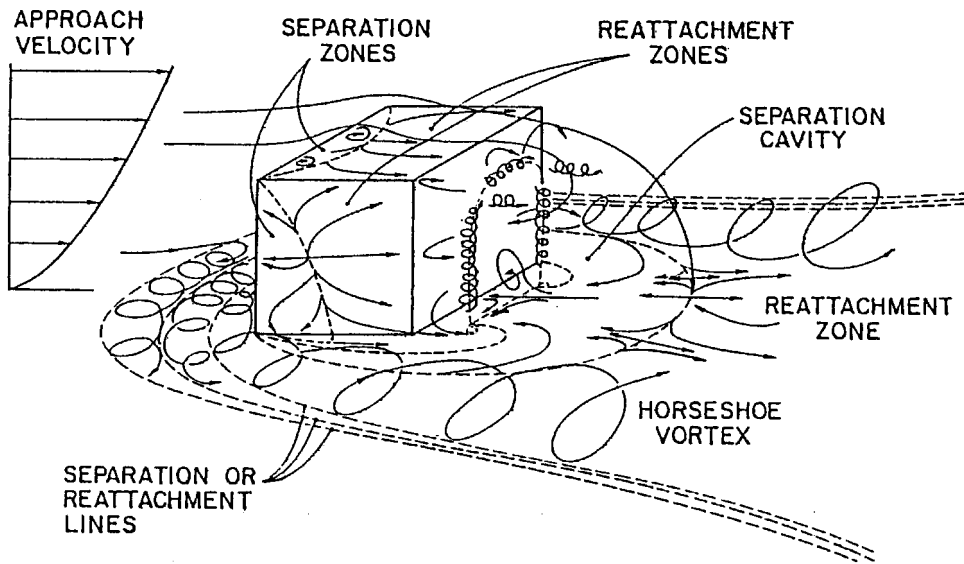


Fig. 14 – Schematic flow field around three-dimensional bluff body.

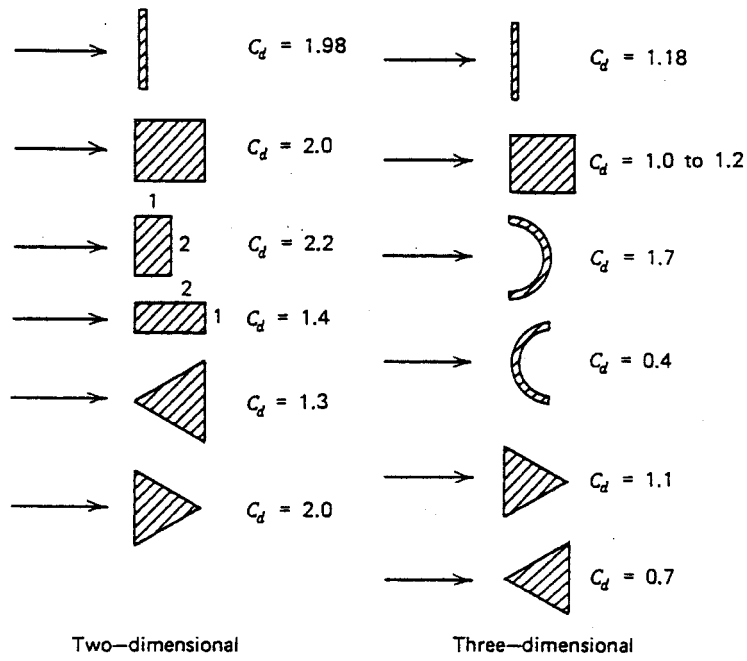


Fig. 15 – Drag coefficients of two-dimensional and three-dimensional bodies

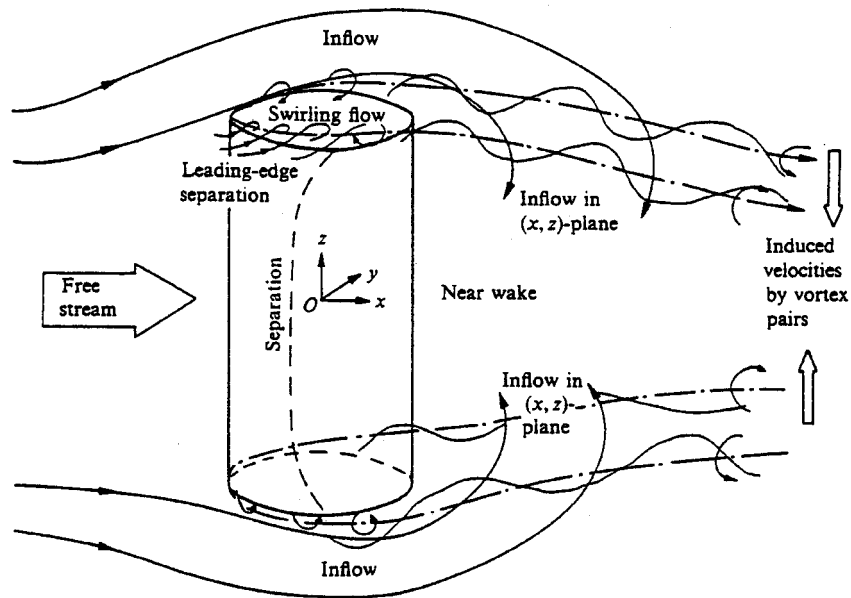


Fig. 16 – Flow around a finite-length cylinder

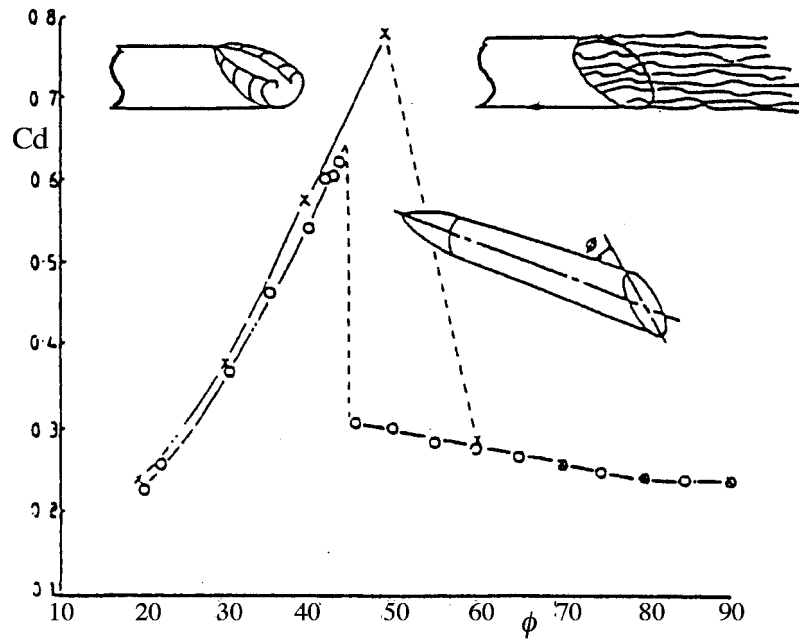


Fig. 17 – Drag coefficient of an axisymmetrical body as a function of base inclination (from Bearman 1980).

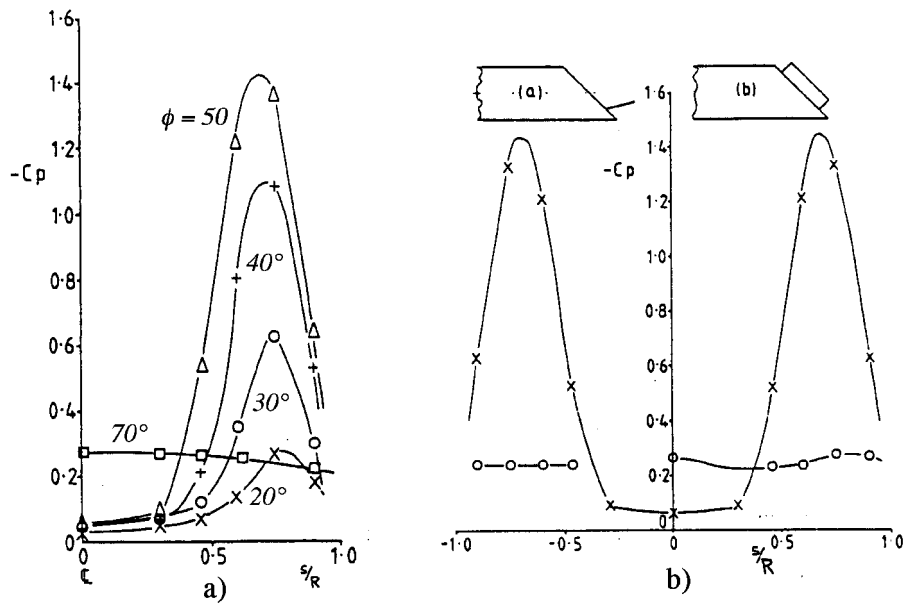


Fig. 18 – Pressure distributions measured along a horizontal line passing through the base center. a) Variation with base angle. b) Effect of disturbing devices for $\phi = 50^\circ$: x – plain; o – with device (from Bearman 1980).

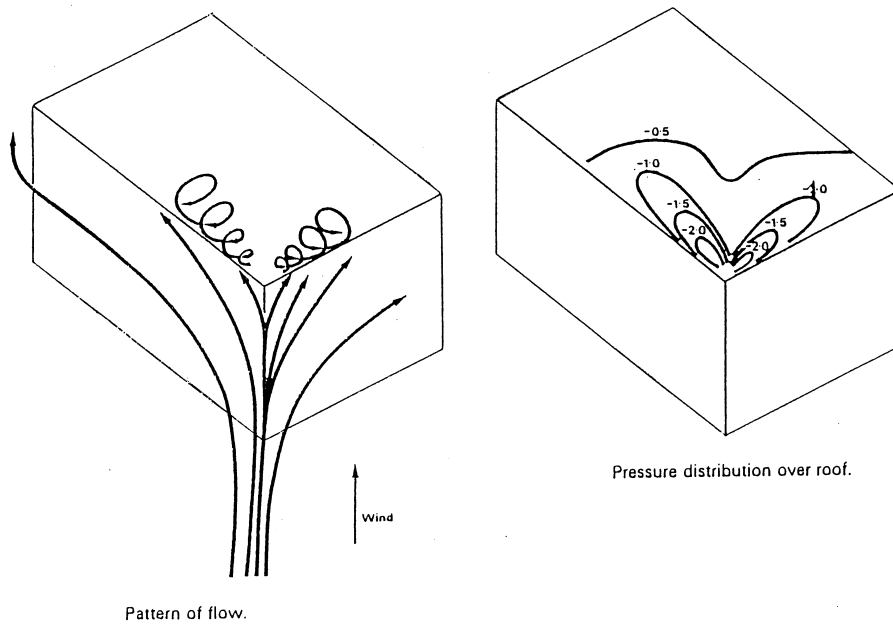


Fig. 19 – Flow patterns and local pressure coefficients on a buiding shape

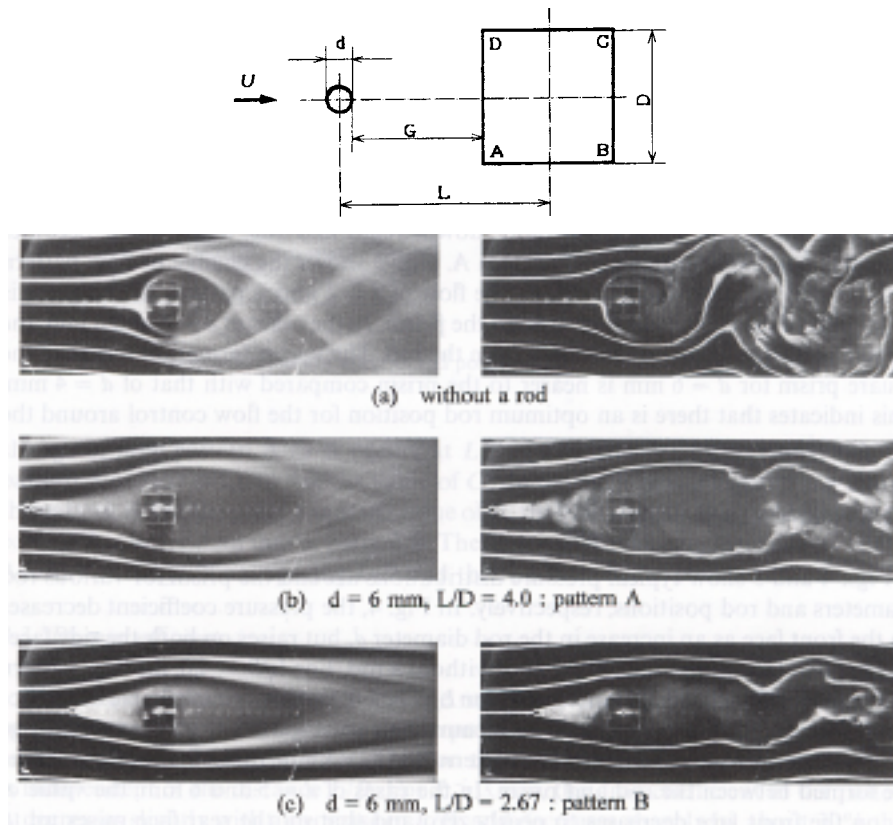


Fig. 20 – Modifications of the mean (left) and instantaneous (right) flow patterns around a square cylinder by a small rod placed upstream in different positions (from Igarashi 1997).

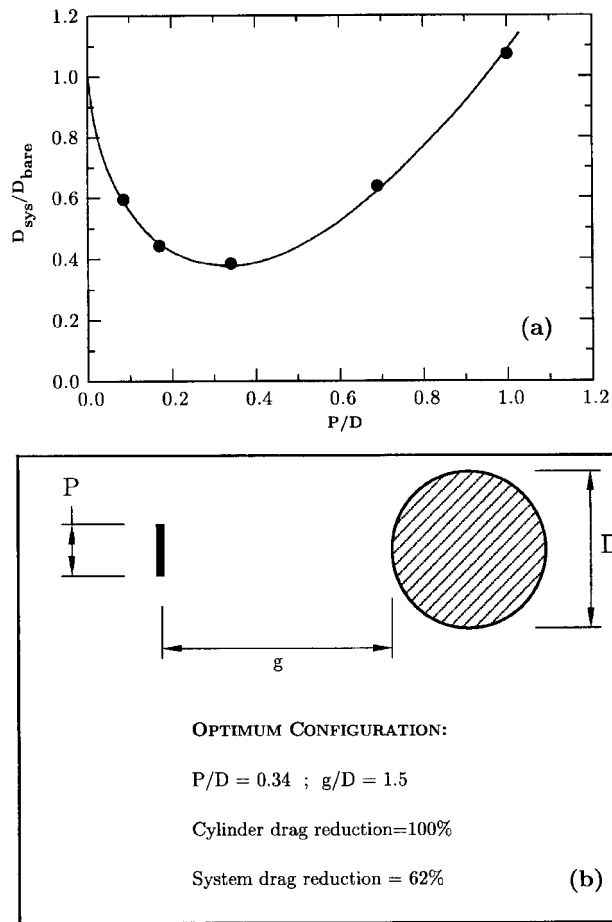


Fig. 21 – Variation of the system drag with size ratio between plate and cylinder (a), and optimal geometrical configuration (b) (from Prasad & Williamson 1997).

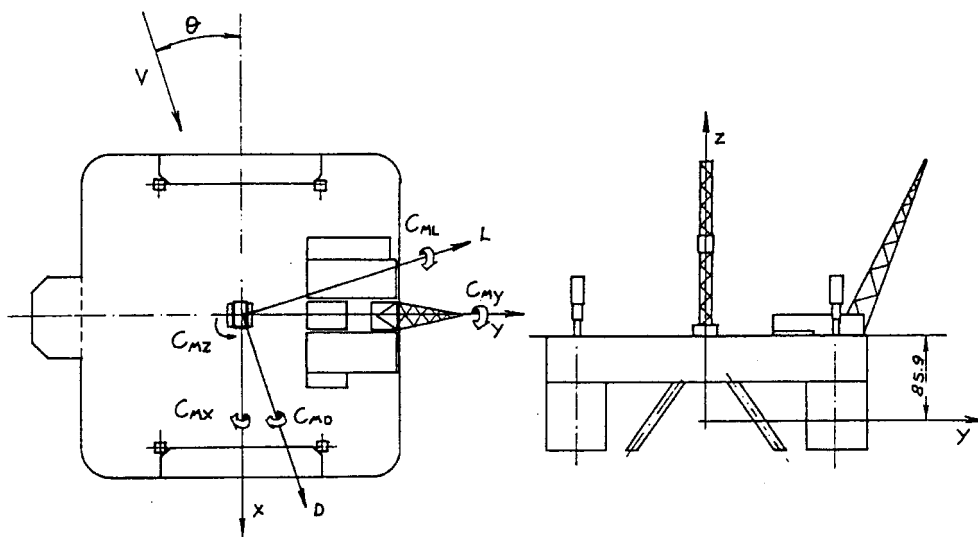


Fig. 22 – Scheme of the model of a tension leg platform (from Buresti et al. 1986).

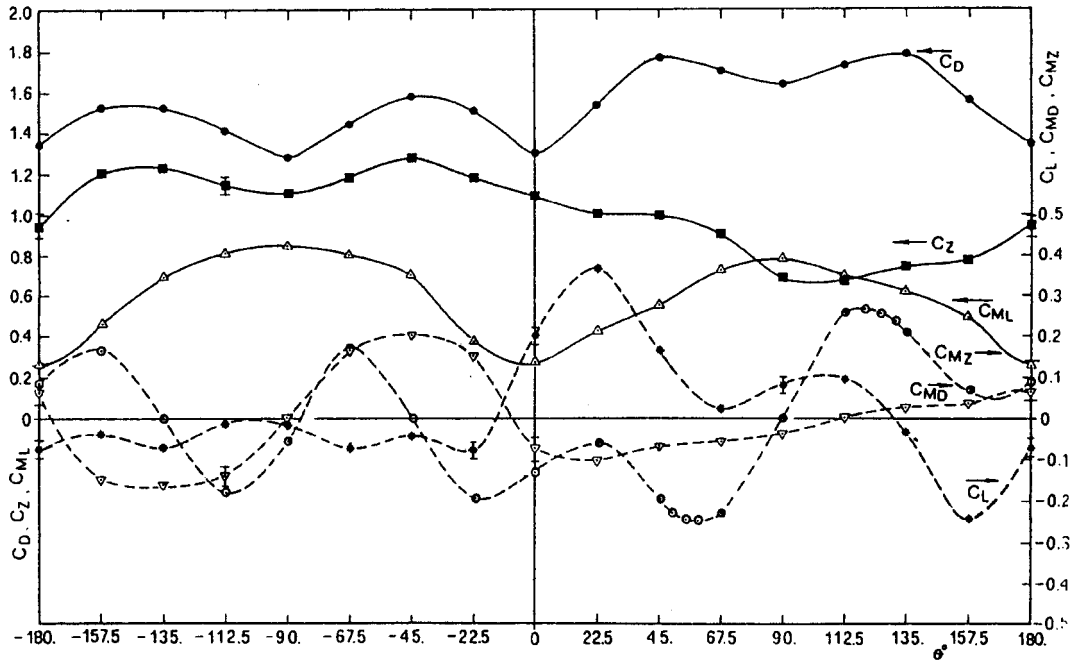


Fig. 23 – Load coefficients obtained in the wind tunnel tests of the model of Fig. 22 (from Buresti et al. 1986).

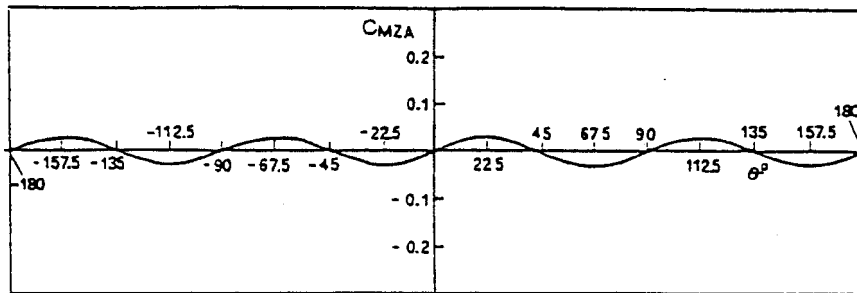


Fig. 24 – Contribution to C_{Mz} from the deck, considered as a prismatic body.

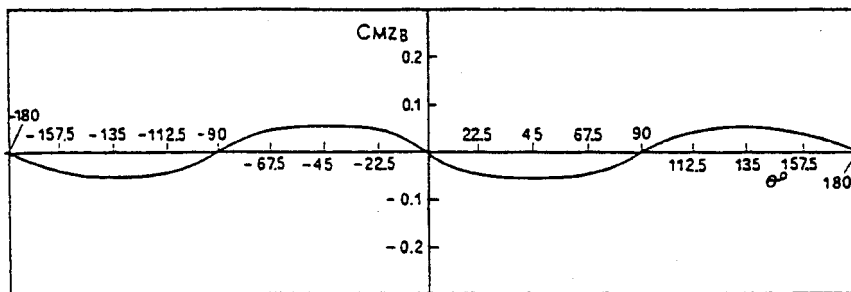


Fig. 25 – Contribution to C_{Mz} from the deck indentation.

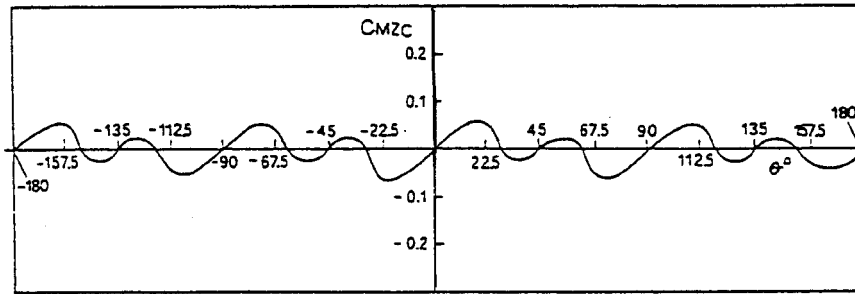


Fig. 26 - Contribution to C_{Mz} from the lateral forces on the columns.

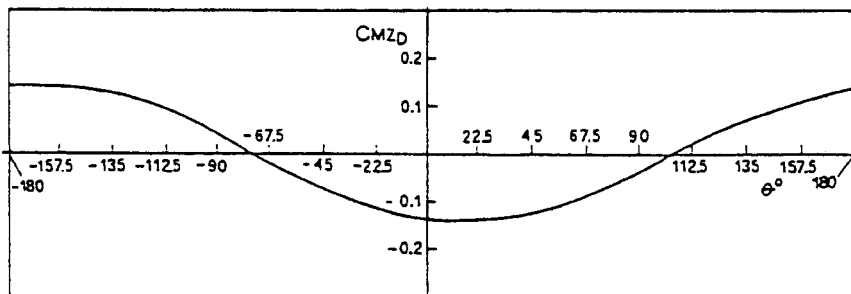


Fig. 27 - Contribution to C_{Mz} from the drag on the bodies over the deck.

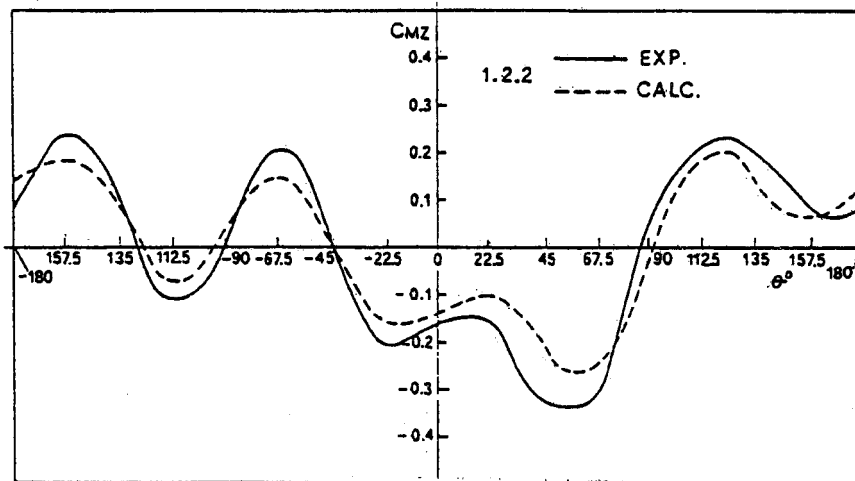


Fig. 28 – Comparison between the predicted and the experimental values of C_{Mz} for the complete model (from Buresti et al. 1986).